Constraints on Covariant Dark-Matter–Nucleon Effective Field Theory Interactions from the First Science Run of the LUX-ZEPLIN Experiment

J. Aalbers,[1,2] D. S. Akerib,[1,2] A. K. Al Musalhi,[3] F. Alder,[3] C. S. Amarasinghe,[4,5] A. Ames,[1,2] T. J. Anderson,[1,6] N. Angelides,[7] H. M. Araújo,[7] J. E. Armstrong,[8] M. Arthurs,[1,6] A. Baker,[7] S. Balashov,[9] J. Bang,[10] E. E. Barillier,[5,11] J. W. Bargemann,[4] K. Beattie,[12] T. Benson,[13] A. Bhatti,[8] A. Biekert,[12,14] T. P. Biesiadzinski,[1,6] H. J. Birch,[5,11] E. J. Bishop,[15] G. M. Blockinger,[16] B. Boxer,[17,*] C. A. J. Brew,[9] P. Brás,[18] S. Burdin,[19] M. Buuck,[1,6] M. C. Carmona-Benitez,[20] M. Carter,[19] A. Chawla,[21] H. Chen,[12] J. J. Cherwinka,[13] Y. T. Chin,[20] N. I. Chott,[22] M. V. Converse,[23] A. Cottle,[3] G. Cox,[24] D. Curran,[24] C. E. Dahl,[25,26] A. David,[3] J. Delgaudio,[24] S. Dey,[27] L. de Viveiros,[20] L. Di Felice,[7] C. Ding,[10] J. E. Y. Dobson,[28] E. Druszkiewicz,[23] S. R. Eriksen,[29,†] A. Fan,[1,6] N. M. Fearon,[27] S. Fiorucci,[12] H. Flaecher,[29] E. D. Fraser,[19] T. M. A. Fruth,[30] R. J. Gaitskell,[10] A. Geffre,[24] J. Genovesi,[22] C. Ghag,[3] R. Gibbons,[12,14] S. Gokhale,[31] J. Green,[27] M. G. D. van der Grinten,[9] J. J. Haiston,[22] C. R. Hall,[8] S. Han,[1,6] E. Hartigan-O'Connor,[10] S. J. Haselschwardt,[12] M. A. Hernandez,[5,11] S. A. Hertel,[32] G. Heuermann,[5] G. J. Homenides,[33] M. Horn,[24] D. Q. Huang,[5] D. Hunt,[27] E. Jacquet,[7] R. S. James,[3,‖] J. Johnson,[17] A. C. Kaboth,[21] A. C. Kamaha,[34] M. Kannichankandy,[16] D. Khaitan,[23] A. Khazov,[9] I. Khurana,[3] J. D. Kim,[35] J. Kim,[4] J. Kingston,[17] R. Kirk,[10] D. Kodroff,[20,12] L. Korley,[5] E. V. Korolkova,[36] H. Kraus,[27] S. Kravitz,[12,37] L. Kreczko,[29] V. A. Kudryavtsev,[36] D. S. Leonard,[35] K. T. Lesko,[12] C. Levy,[16] J. Lin,[12,14] A. Lindote,[18] R. Linehan,[1,6] W. H. Lippincott,[4] M. I. Lopes,[18] W. Lorenzon,[5] C. Lu,[10] S. Luitz,[1] P. A. Majewski,[9] A. Manalaysay,[12] R. L. Mannino,[38] C. Maupin,[24] M. E. McCarthy,[23] G. McDowell,[5] D. N. McKinsey,[12,14] J. McLaughlin,[25] J. B. McLaughlin,[3] R. McMonigle,[16] E. H. Miller,[1,6] E. Mizrachi,[8,38] A. Monte,[4] M. E. Monzani,[1,6,39] J. D. Morales Mendoza,[1,6] E. Morrison,[22] B. J. Mount,[40] M. Murdy,[32] A. St. J. Murphy,[15] A. Naylor,[36] H. N. Nelson,[4] F. Neves,[18] A. Nguyen,[15] J. A. Nikoleyczik,[13] I. Olcina,[12,14] K. C. Oliver-Mallory,[7] J. Orpwood,[36] K. J. Palladino,[27] J. Palmer,[21] N. J. Pannifer,[29] N. Parveen,[16] S. J. Patton,[12] B. Penning,[5,11] G. Pereira,[18] E. Perry,[3] T. Pershing,[38] A. Piepke,[33] Y. Qie,[23] J. Reichenbacher,[22] C. A. Rhyne,[10] Q. Riffard,[12] G. R. C. Rischbieter,[5,11] H. S. Riyat,[15] R. Rosero,[31] T. Rushton,[36] D. Rynders,[24] D. Santone,[21] A. B. M. R. Sazzad,[33] R. W. Schnee,[22] S. Shaw,[15] T. Shutt,[1,6] J. J. Silk,[8] C. Silva,[18] G. Sinev,[22] J. Siniscalco,[3] R. Smith,[12,14] V. N. Solovov,[18] P. Sorensen,[12] J. Soria,[12,14] I. Stancu,[33] A. Stevens,[3,7] K. Stifter,[26] B. Suerfu,[12,14] T. J. Sumner,[7] M. Szydagis,[16] W. C. Taylor,[10] D. R. Tiedt,[24] M. Timalsina,[12,22] Z. Tong,[7] D. R. Tovey,[36] J. Tranter,[36] M. Trask,[4] M. Tripathi,[17] D. R. Tronstad,[22] A. Vacheret,[7] A. C. Vaitkus,[10] O. Valentino,[7] V. Velan,[12] A. Wang,[1,6] J. J. Wang,[33] Y. Wang,[12,14] J. R. Watson,[12,14] R. C. Webb,[41] L. Weeldreyer,[33] T. J. Whitis,[4] M. Williams,[5,12,‡] W. J. Wisniewski,[1] F. L. H. Wolfs,[23] S. Woodford,[19] D. Woodward,[20,12] C. J. Wright,[31,§] Q. Xia,[12] X. Xiang,[10,31] J. Xu,[38] M. Yeh,[31] and E. A. Zweig[34]

(LZ Collaboration)

[1]*SLAC National Accelerator Laboratory, Menlo Park, California 94025-7015, USA*
[2]*Kavli Institute for Particle Astrophysics and Cosmology, Stanford University, Stanford, California 94305-4085, USA*
[3]*University College London (UCL), Department of Physics and Astronomy, London WC1E 6BT, United Kingdom*
[4]*University of California, Santa Barbara, Department of Physics, Santa Barbara, California 93106-9530, USA*
[5]*University of Michigan, Randall Laboratory of Physics, Ann Arbor, Michigan 48109-1040, USA*
[6]*Kavli Institute for Particle Astrophysics and Cosmology, Stanford University, Stanford, California 94305-4085 USA*
[7]*Imperial College London, Physics Department, Blackett Laboratory, London SW7 2AZ, United Kingdom*
[8]*University of Maryland, Department of Physics, College Park, Maryland 20742-4111, USA*
[9]*STFC Rutherford Appleton Laboratory (RAL), Didcot OX11 0QX, United Kingdom*
[10]*Brown University, Department of Physics, Providence, Rhode Island 02912-9037, USA*
[11]*University of Zurich, Department of Physics, 8057 Zurich, Switzerland*
[12]*Lawrence Berkeley National Laboratory (LBNL), Berkeley, California 94720-8099, USA*
[13]*University of Wisconsin-Madison, Department of Physics, Madison, Wisconsin 53706-1390, USA*
[14]*University of California, Berkeley, Department of Physics, Berkeley, California 94720-7300, USA*
[15]*University of Edinburgh, SUPA, School of Physics and Astronomy, Edinburgh EH9 3FD, United Kingdom*
[16]*University at Albany (SUNY), Department of Physics, Albany, New York 12222-0100, USA*
[17]*University of California, Davis, Department of Physics, Davis, California 95616-5270, USA*
[18]*Laboratório de Instrumentação e Física Experimental de Partículas (LIP), University of Coimbra, P-3004 516 Coimbra, Portugal*
[19]*University of Liverpool, Department of Physics, Liverpool L69 7ZE, United Kingdom*

[20]Pennsylvania State University, Department of Physics, University Park, Pennsylvania 16802-6300, USA
[21]Royal Holloway, University of London, Department of Physics, Egham TW20 0EX, United Kingdom
[22]South Dakota School of Mines and Technology, Rapid City, South Dakota 57701-3901, USA
[23]University of Rochester, Department of Physics and Astronomy, Rochester, New York 14627-0171, USA
[24]South Dakota Science and Technology Authority (SDSTA), Sanford Underground Research Facility, Lead, South Dakota 57754-1700, USA
[25]Northwestern University, Department of Physics & Astronomy, Evanston, Illinois 60208-3112, USA
[26]Fermi National Accelerator Laboratory (FNAL), Batavia, Illinois 60510-5011, USA
[27]University of Oxford, Department of Physics, Oxford OX1 3RH, United Kingdom
[28]King's College London, Department of Physics, London WC2R 2LS, United Kingdom
[29]University of Bristol, H.H. Wills Physics Laboratory, Bristol BS8 1TL, United Kingdom
[30]The University of Sydney, School of Physics, Physics Road, Camperdown, Sydney, NSW 2006, Australia
[31]Brookhaven National Laboratory (BNL), Upton, New York 11973-5000, USA
[32]University of Massachusetts, Department of Physics, Amherst, Massachusetts 01003-9337, USA
[33]University of Alabama, Department of Physics & Astronomy, Tuscaloosa, Alabama 34587-0324, USA
[34]University of Califonia, Los Angeles, Department of Physics & Astronomy, Los Angeles, Califonia 90095-1547, USA
[35]IBS Center for Underground Physics (CUP), Yuseong-gu, Daejeon, Korea
[36]University of Sheffield, Department of Physics and Astronomy, Sheffield S3 7RH, United Kingdom
[37]University of Texas at Austin, Department of Physics, Austin, Texas 78712-1192, USA
[38]Lawrence Livermore National Laboratory (LLNL), Livermore, California 94550-9698, USA
[39]Vatican Observatory, Castel Gandolfo, V-00120, Vatican City State
[40]Black Hills State University, School of Natural Sciences, Spearfish, South Dakota 57799-0002, USA
[41]Texas A&M University, Department of Physics and Astronomy, College Station, Texas 77843-4242, USA

(Received 30 April 2024; revised 10 September 2024; accepted 15 October 2024; published 26 November 2024)

The LUX-ZEPLIN (LZ) experiment is a dual-phase xenon time project chamber operating in the Sanford Underground Research Facility in South Dakota, USA. We report on the results of a relativistic extension to the nonrelativistic effective field theory (NREFT) from a 5.5 t fiducial mass and 60 live days of exposure. We present constraints on couplings from covariant interactions arising from the coupling of vector, axial currents, and electric dipole moments of the nucleon to the magnetic and electric dipole moments of the weakly interacting massive particle which cannot be described by recasting previous results described by an NREFT. Using a profile-likelihood ratio analysis, in an energy region between 0 keV_{nr} to 270 keV_{nr}, we report 90% confidence level exclusion limits on the coupling strength of five interactions in both the isoscalar and isovector bases.

DOI: 10.1103/PhysRevLett.133.221801

Introduction—The current generation of dark matter (DM) direct detection experiments, searching for weakly interacting massive particles (WIMPs), such as LZ [1], XENONnT [2], and PandaX [3], have already probed a large parameter space for WIMPs. These experiments have typically focused on spin-independent (SI) and spin-dependent (SD) WIMP-nucleon interactions with WIMP masses of a few GeV/c^2 to tens of TeV/c^2. The recent null results from both LZ [4] and XENONnT [2] motivate the need to investigate other models.

Using an effective field theory (EFT), such as that developed by Fan *et al.* [5] and Fitzpatrick *et al.* [6], it is possible to probe a wide variety of dark matter interactions and parameters in a model-independent way. It is possible to produce a complete set of effective operators that describe the possible interactions between WIMPs and standard model (SM) particles, making it an attractive way to increase the potential sensitivity of direct detection experiments beyond the standard SI and SD interactions. A nonrelativistic effective field theory (NREFT) framework has already been used to probe some of the potential interactions, such as in LUX [7], XENON1T [8], PandaX-II [9], and LZ [10]. The operators in this NREFT can be mapped onto covariant Lagrangians, via a nonrelativistic reduction of the relativistic fields, allowing for more complex interactions to be studied [5,6]. Specifically,

*Contact author: bboxer@ucdavis.edu
†Contact author: sam.eriksen@bristol.ac.uk
‡Contact author: michrw@umich.edu
§Contact author: christopher.wright@bristol.ac.uk
‖Present address: The University of Melbourne, School of Physics, Melbourne, VIC 3010, Australia.

since these Lagrangians are relativistic, they are powerful probes of potential WIMP interactions, parameters, and structure in a way previous NREFT, SI, and SD studies are not.

In this Letter, we perform a search for signals arising from five covariant SD Lagrangians that describe possible interactions between WIMPs and nucleons. The interactions studied give insight into the potential millicharged nature of the WIMP [11]. In this case, the WIMP can be composed of multiple charged particles, or be a fundamental particle with charge itself. We analyze data taken by the LZ experiment during its first science run using an extended energy window, previously described in Ref. [10], and perform a statistical analysis to constrain the coefficients associated with each Lagrangian.

Theory—SD interactions between the WIMP and nucleon can be comprised of WIMP magnetic and electric dipole moments, axial-vector interference terms, and tensor interactions in addition to the standard SD physics previously studied. In this analysis, we focus on spin-1/2 WIMPs where interactions with the target nucleus are of dimension 5 or higher, following what has been described by Anand *et al.* [12]. The energy scale of these interactions is set by the maximum momentum transfer of ∼200 MeV, which is determined through considerations of the WIMP mass and escape velocity. WIMP-nucleon interactions are constructed from the available bilinear products of scalar and four-vector interactions resulting in $2^2 + 4^2 = 20$ separate interaction Lagrangians. These consist of six main interaction types: scalar, pseudoscalar, vector, axial vector, magnetic moment, and electric dipole moment interactions. In this analysis, we only consider Lagrangians that incorporate electric dipole, covariant vector, or a magnetic moment coupling component in the interaction, shown in the rightmost column of Table I.

A nonrelativistic reduction is done between the covariant Lagrangian and the NREFT operators by replacing the spinors in the fields with the low-momentum counterparts following the prescription in Ref. [12]. When using the NREFT, we consider a four-body covariant interaction between the WIMP and the nucleon described by a Lagrangian

$$\mathcal{L}^j_{\rm int} = d_j \bar{\chi} \mathcal{O}^j_\chi \chi \bar{N} \mathcal{O}^j_N N, \tag{1}$$

where j is an index of the Lagrangian and d_j is the dimensionless coupling to be determined by the experiment that measures the effective strength or size of the interaction. $\bar{\chi}$, χ, $\bar{N}$, and N represent the nonrelativistic fields of the dark matter candidate particle and nuclear targets. $\mathcal{O}_\chi$ and $\mathcal{O}_N$ are the nonrelativistic WIMP and nucleon operators described in Ref. [12]. To write our covariant interaction in terms of this NREFT we can take for example $\mathcal{L}_{10}$:

$$\mathcal{L}_{10} = \bar{\chi} i\sigma^{\mu\nu} \frac{q_\nu}{m_M} \chi \bar{N} i\sigma_{\mu\alpha} \frac{q^\alpha}{m_M} N. \tag{2}$$

The leading terms come from the spatial components, so we can make the following transformations: $\gamma^\mu \to \gamma^i$ and $\sigma^\mu \to \sigma^i$. We then define *dimension* as 4+ number of powers of m_M in the denominator of the covariant interactions seen in Table I, where m_M is a normalization parameter introduced to normalize interaction to a dimensionless value. Given then that the relationship between particle spin and the Pauli matrix is defined as $\sigma^i = 2S^i$, we can transform Eq. (2) into

$$\mathcal{L}_{10} = 4\left(\frac{\vec{q}}{m_M} \times \overrightarrow{S_\chi}\right) \cdot \left(\frac{\vec{q}}{m_M} \times \overrightarrow{S_N}\right). \tag{3}$$

From Ref. [12] we can retrieve that $\mathcal{O}_4 = \overrightarrow{S_\chi} \cdot \overrightarrow{S_N}$ and $\mathcal{O}_6 = [\overrightarrow{S_\chi} \cdot (\vec{q}/m_N)][\overrightarrow{S_N} \cdot (\vec{q}/m_N)]$ and rearrange Eq. (3) to find the reduced form of the interaction as

$$\mathcal{L}_{10} = 4\left(\frac{\vec{q}^2}{m_M^2}\mathcal{O}_4 - \frac{m_N^2}{m_M^2}\mathcal{O}_6\right). \tag{4}$$

We adopt this nonrelativistic reduction for our analysis as it enables us to use existing nuclear shell model calculations when computing recoil spectra. Similar steps are taken to relativistically match nonlinear combinations of the NREFT operators to the other covariant interactions of interest. The reduced Lagrangians written in terms of the operators can be seen in the center column of Table I.

TABLE I. Interactions considered in this analysis, with j referring to the numerical index of the specific Lagrangian, out of the total possible 20. For each Lagrangian, the relation to the NREFT operators ($\mathcal{O}$) is given in addition to the interaction that is generated [5,6]. Lagrangians: vector (Ve), electric dipole (ED) and magnetic moment (MM).

j	$\mathcal{L}^j_{\rm int}$	$\Sigma_i c_i \mathcal{O}_i$	WIMP-Nucleon interaction
6	$\bar{\chi}\gamma^\mu\chi\bar{N}i\sigma_{\mu\alpha}(q^\alpha/m_M)N$	$(\vec{q}^2/2m_N m_M)\mathcal{O}_1 - 2(m_N/m_{\rm M})\mathcal{O}_3 + 2(m_N^2/m_M m_\chi)[(q^2/m_N^2)\mathcal{O}_4 - \mathcal{O}_6]$	Ve-MM
9	$\bar{\chi}i\sigma^{\mu\nu}(q_\nu/m_M)\chi\bar{N}\gamma_\mu N$	$(\vec{q}^2/2m_\chi m_M)\mathcal{O}_1 + (2m_N/m_M)\mathcal{O}_5 - 2(m_N/m_M)[(\vec{q}^2/m_N^2)\mathcal{O}_4 - \mathcal{O}_6]$	MM-Ve
10	$\bar{\chi}i\sigma^{\mu\nu}(q_\nu/m_M)\chi\bar{N}i\sigma_{\mu\alpha}(q^\alpha/m_M)N$	$4[(\vec{q}^2/m_M^2)\mathcal{O}_4 - (m_N^2/m_M^2)\mathcal{O}_6]$	MM-MM
12	$i\bar{\chi}i\sigma^{\mu\nu}(q_\nu/m_M)\chi\bar{N}i\sigma_{\mu\alpha}(q^\alpha/m_M)\gamma^5 N$	$-(m_N/m_\chi)(\vec{q}^2/m_{\rm M}^2)\mathcal{O}_{10} - 4(\vec{q}^2/m_{\rm M}^2)\mathcal{O}_{12} - 4(m_N^2/m_{\rm M}^2)\mathcal{O}_{15}$	MM-ED
18	$i\bar{\chi}i\sigma^{\mu\nu}(q_\nu/m_M)\gamma^5\chi N i\sigma_{\mu\alpha}(q^\alpha/m_M)N$	$(\vec{q}^2/m_{\rm M}^2)\mathcal{O}_{11} + 4(m_N^2/m_{\rm M}^2)\mathcal{O}_{15}$	ED-MM

None of the interactions presented in this analysis can be obtained from simple linear reordering of NREFT operators. This is because in the reduced form, each operator term contains differing dependence on momentum transfer $\vec{q}$. Differing powers of $\vec{q}$ prevent obtaining the Lagrangian result from the limits determined by previous work finding coefficients for each operator alone, as in Ref. [10]. This work therefore probes dark matter interactions beyond that of determining operator coefficients in isolation.

Interactions are normalized to a dimensionless value by including the term m_M in the denominator of all momentum terms. The m_M term is set equal to the nucleon mass m_N, normalizing the WIMP and nucleon momentum to the nucleon scale, as this is the natural scale for a theory dealing with nucleon interactions. This choice allows us to extract information such as the size of the WIMP magnetic or electric dipole moments from the measurement of the dimensionless coupling parameter d_j.

LZ detector—The LZ experiment, located in the Davis Campus of the Sanford Underground Research Facility, in South Dakota, USA, is centered around a low-background dual-phase time project chamber (TPC) detector containing 7 tonnes of liquid xenon (LXe) in the sensitive volume [1,13]. The cylindrical TPC is equipped with an array of photomultiplier tubes (PMTs) at the top and bottom of the detector. These PMTs detect the energy depositions in the detector that typically make two signals. The first is prompt scintillation light (S1) and the second is a delayed signal (S2) caused by the electroluminescent light that occurs when electrons reach the top of the detector due to an electric field. The TPC is surrounded by an active LXe Skin veto detector that tags gamma-ray photons entering or exiting the TPC. Enclosing the entire cryostat is the outer detector (OD), which is composed of 17 tonnes of Gd-loaded liquid scintillator and 238 tonnes of ultrapure water to detect neutrons and muons.

The dataset used for this analysis was collected between December 2021 and May 2022 and corresponds to a total live time of 60 days with a fiducial mass of 5.5 tonnes. The detector condition during this period is detailed in Refs. [4,10]. The validation of the response of the detector to nuclear recoil (NR) and electron recoil (ER) recoil events, as well as the determination of the position-corrected S1 and S2 ($S1_c$ and $S2_c$) scaling factors, is performed using calibration data and NEST 2.3.7 [14,15] as outlined in Ref. [10].

Analysis—The couplings of each Lagrangian are explored using the first science run of LZ in an extended energy region, as previously used in Ref. [10]. An unbinned frequentist profile likelihood ratio test is performed between background and signal plus background in the ($S1_c$, $\log_{10}(S2_c)$) observable space. $S1_c$ is constrained between 3 and 600 photoelectrons (phd) and $\log_{10}(S2_c) \leq 4.5$, mirroring the range used in Ref. [10].

The backgrounds in the dataset, estimated in Ref. [10], are dominated by a flat-ER component comprised of ^{212}Pb, ^{214}Pb, and ^{85}Kr. Other contributions to the ER background are ^{37}Ar, ^{124}Xe, ^{127}Xe, ^{136}Xe, ^{125}I, solar neutrinos, and Compton scatters from detector components. The NR backgrounds considered are from ^{8}B coherent neutrino-nucleus scattering and the scattering of neutrons originating from detector materials. The best-fit values for each is less than one [10]. Additionally, uncorrelated S1 and S2 pulses that may pair into accidental single scatter pairs are considered.

The recoil spectrum for each Lagrangian is generated using WimPyDD [16] with modified Xe one-body nuclear

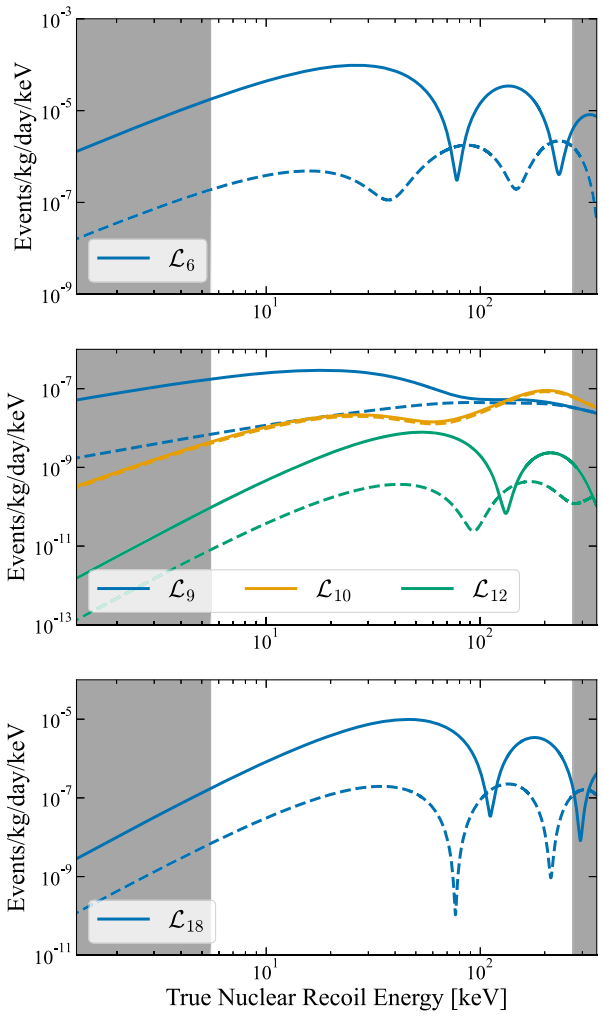

FIG. 1. Differential recoil spectra from the five covariant WIMP-nucleon Lagrangians considered in this analysis. Shown are the isoscalar (solid line) and isovector (dashed line) for a 1000 GeV/c^2 WIMP. The Lagrangians are categorized by the WIMP interaction: vector (top), magnetic moment (middle), and electric dipole (bottom) interactions. The spectra were generated with a dimensionless coupling strength of unity. The shaded gray regions indicate the energies at which the detection efficiency is below 50% after all data analysis cuts have been applied (as described in Ref. [10]).

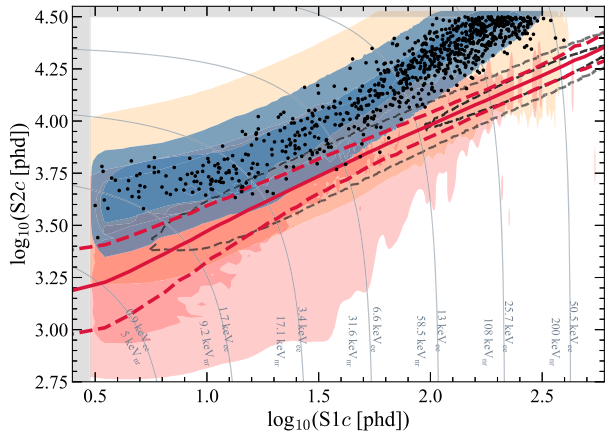

FIG. 2. The final high energy WIMP-search data after all cuts in $\{\log_{10}(\mathrm{S1}c), \log_{10}(\mathrm{S2}c)\}$ space. The contours that enclose 1σ (dark) and 2.5σ (light) regions represent the following models: the shaded red region indicates neutrons originating from detector materials, the shaded orange region indicates Compton scatters from detector components, the blue region is the combined representation of all other ER models (^{214}Pb, ^{212}Pb, ^{85}Kr, ^{37}Ar, ^{125}I, ^{124}Xe, ^{127}Xe, ^{136}Xe, and ν ER), and the black dashed lines show a 1000 GeV/c^2 $\mathcal{L}_6$ isoscalar signal model. The solid red line corresponds to the NR median, while the red dotted lines represent the 10%–90% percentiles. The model contours are produced with a linear scale for $\mathrm{S1}_c$ prior to being plotted on a log scale and take into account all the efficiencies used in the analysis. Contours of constant recoil energy have been included as thin gray lines. Grayed regions at the left and top of the plot indicate parameter space outside the energy region of interest.

density matrices to take into account more up to date calculations [17,18]. Following the convention set in Ref. [19], the WIMP velocity distribution, $f(v)$, is described by the standard halo model with $\vec{v}_{\circledast} = (11.1, 12.2, 7.3)$ km/s (solar peculiar velocity) [20], $\vec{v}_0 = (0, 238, 0)$ km/s (local standard of rest velocity) [21,22], and $v_{\mathrm{esc}} = 544$ km/s (galactic escape speed) [23]. The local DM density, ρ_0, is taken as 0.3 GeV/cm^3 [24]. Figure 1 shows the differential rate spectra for a 1000 GeV/c^2 WIMP-nucleon isoscalar interaction for each Lagrangian considered in this analysis. We consider both isoscalar and isovector bases to allow future comparison with experiments with potentially different target nuclei.

Figure 2 shows the $\{\log_{10}(\mathrm{S1}c), \log_{10}(\mathrm{S2}c\}$ distribution of the 835 events which pass all selections, along with contours representing a 1000 GeV/c^2 $\mathcal{L}_6$ isoscalar signal model (representative of signal models that peak at nonzero energy), and the background model.

Results—No significant evidence of an excess is found in either the isoscalar or isovector bases. Unbinned Kolmogorov-Smirnov tests comparing the reconstructed energy distributions of the data and the background-only model give p values of 0.392. This shows consistency with the background-only scenario for all Lagrangians and WIMP masses tested. The interaction coupling parameters, d_j, for $\mathcal{L}_{6,9,10,12,18}$ are constrained, and shown in Figs. 3 and 4. Where available, previous limits on Lagrangians from PandaX-II [9] are shown for comparison. Each limit has a power constraint applied, such that the probability of excluding any d_j coupling strength, if the background-only hypothesis is true, is not less than 0.16. This restricts the upper limit from dropping below 1σ of the median expectation due to underfluctuations in the data [19].

The shape of each limit, and therefore the corresponding mass of maximum sensitivity, varies with the expected rate of events seen in the recoil spectra, shown in Fig. 1. Thus, Lagrangians with rates that increase at higher mass will have maximum sensitivity at higher mass. At masses above

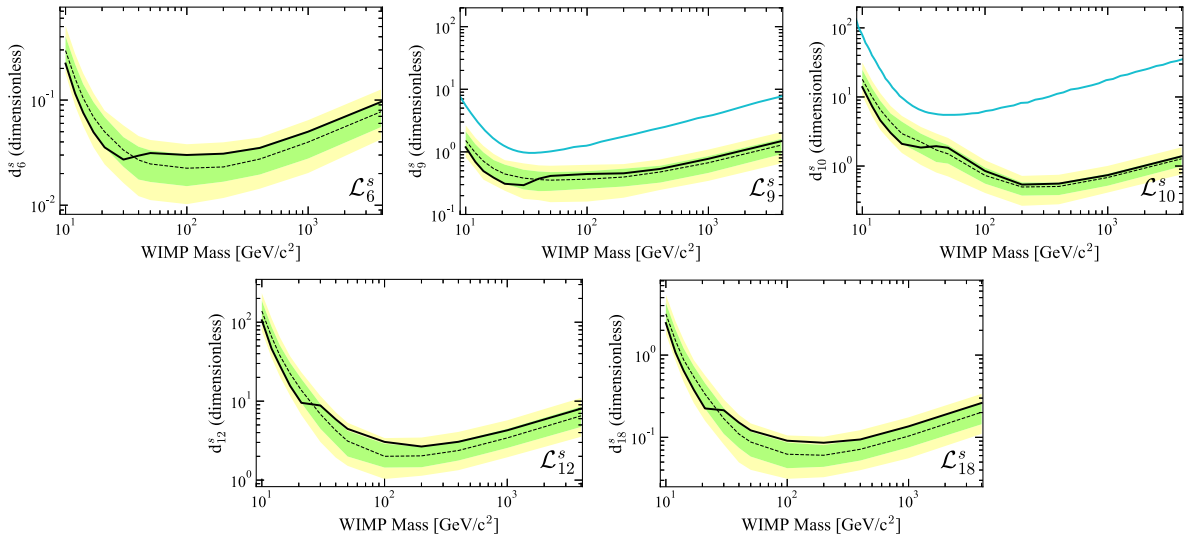

FIG. 3. The 90% confidence limit (black lines) on the dimensionless isoscalar interaction couplings d_j for each of the five interactions. The black dotted lines show the medians of the sensitivity projection, and the green and yellow bands correspond to the 1σ and 2σ sensitivity bands, respectively. Also shown are the results from PandaX-II experiment in blue where available [9].

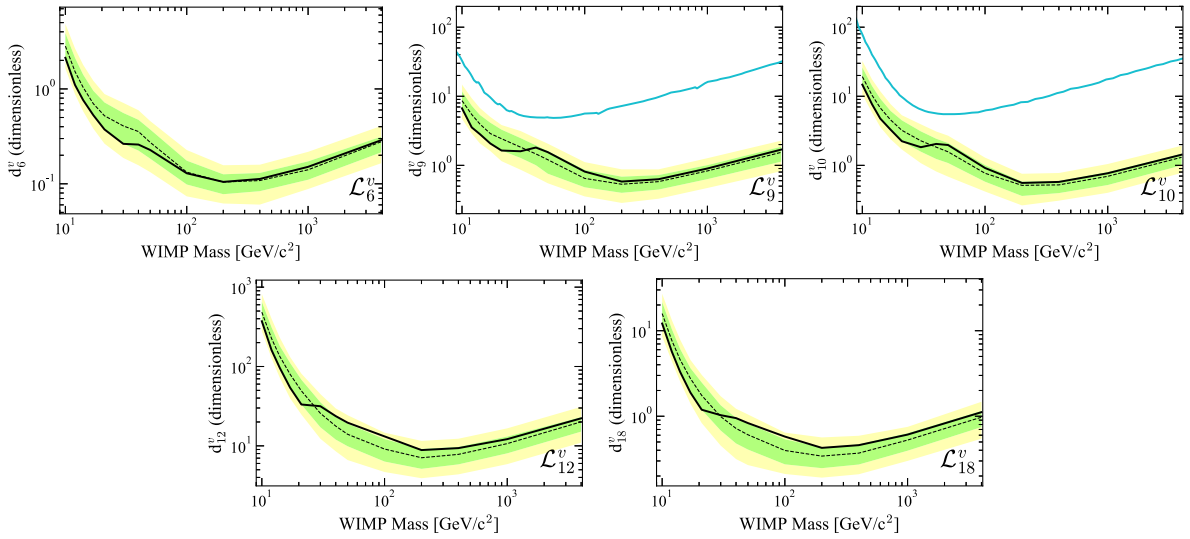

FIG. 4. The 90% confidence limit (black lines) on the dimensionless isovector interaction couplings d_j for each of the five interactions. The black dotted lines show the medians of the sensitivity projection, and the green and yellow bands correspond to the 1σ and 2σ sensitivity bands, respectively. Also shown are the results from PandaX-II experiment in blue where available [9].

30 GeV/c^2, some Lagrangians show limits weaker than the median expectation. This is due to the measured overfluctation of events in the NR band. These events can be seen as the data points that fall below the blue 2.5σ contours of the ER band in Fig. 2. However, all of these events are consistent with ER leakage as described in Refs. [4,10].

The lower bounds of each Lagrangians are near, or below in the case of $\mathcal{L}_6$, the nominal weak scale where $d_j \approx 1$. These results give us information on the absolute size of the WIMP magnetic and electric dipole moment and their coupling to nucleons since we have normalized to the scale of the nucleon ($m_M = m_N$). A data release for this result is in the Supplemental Material [25].

Conclusion—This Letter presents the results of a search for covariant vector, electric dipole moment, and magnetic dipole moment interactions between a WIMP and a nucleon. Ten different interaction nuclear recoil spectra were generated using relativistically matched NREFT operators. Using a frequentist statistical analysis between data and model, no excess is observed for any model. Limits on the interaction coupling strength, d_j, were placed, for masses between 9 GeV/c^2 and 4000 GeV/c^2 for isoscalar and isovector interactions. This work places the strongest constraints to date for every model tested. These results help elucidate possible physics that may explain the behavior of the WIMP and its interactions with SM particles.

Acknowledgments—The research supporting this work took place in part at the Sanford Underground Research Facility (SURF) in Lead, South Dakota. Funding for this work is supported by the U.S. Department of Energy, Office of Science, Office of High Energy Physics under Contracts No. DE-AC02-05CH11231, No. DE-SC0020216, No. DE-SC0012704, No. DE-SC0010010, No. DE-AC02-07CH11359, No. DE-SC0012161, No. DE-SC0015910, No. DE-SC0014223, No. DE-SC0010813, No. DE-SC0009999, No. DE-NA0003180, No. DE-SC0011702, No. DE-SC0010072, No. DE-SC0015708, No. DE-SC0006605, No. DE-SC0008475, No. DE-SC0019193, No. DE-FG02-10ER46709, No. UW PRJ82AJ, No. DE-SC0013542, No. DE-AC02-76SF00515, No. DE-SC0018982, No. DE-SC0019066, No. DE-SC0015535, No. DE-SC0019319, No. DE-SC0024225, No. DE-SC0024114, No. DE-AC52-07NA27344, and No. DOE-SC0012447. This research was also supported by the U.S. National Science Foundation (NSF); the UKRI's Science & Technology Facilities Council under Awards No. ST/M003744/1, No. ST/M003655/1, No. ST/M003639/1, No. ST/M003604/1, No. ST/M003779/1, No. ST/M003469/1, No. ST/M003981/1, No. ST/N000250/1, No. ST/N000269/1, No. ST/N000242/1, No. ST/N000331/1, No. ST/N000447/1, No. ST/N000277/1, No. ST/N000285/1, No. ST/S000801/1, No. ST/S000828/1, No. ST/S000739/1, No. ST/S000879/1, No. ST/S000933/1, No. ST/S000844/1, No. ST/S000747/1, No. ST/S000666/1, No. ST/R003181/1, No. ST/W000547/1, No. ST/W000636/1, and No. ST/W000490/1; the Portuguese Foundation for Science and Technology (FCT) under Award No. PTDC/FIS-PAR/2831/2020; the Institute for Basic Science, Korea (Budget No. IBS-R016-D1); the Swiss National Science Foundation (SNSF) under Award No. 10001549. This research was supported by the Australian Government through the Australian Research Council Centre of Excellence for Dark Matter Particle Physics under Award No. CE200100008. We acknowledge additional support from the STFC Boulby Underground Laboratory in the U.K., the GridPP [26,27] and IRIS

Collaborations, in particular at Imperial College London, the University College London (UCL) Cosmoparticle Initiative, the University of Zurich, and the Center for the Fundamental Physics of the Universe, Brown University. K. T. L. acknowledges the support of Brasenose College and Oxford University. The LZ Collaboration acknowledges the key contributions of Dr. Sidney Cahn, Yale University, in the production of calibration sources. This research used resources of the National Energy Research Scientific Computing Center, a DOE Office of Science User Facility supported by the Office of Science of the U.S. Department of Energy under Contract No. DE-AC02-05CH11231. We gratefully acknowledge support from GitLab through its GitLab for Education Program. The University of Edinburgh is a charitable body, registered in Scotland, with the registration number SC005336. The assistance of SURF and its personnel in providing physical access and general logistical and technical support is acknowledged. We acknowledge the South Dakota Governor's office, the South Dakota Community Foundation, the South Dakota State University Foundation, and the University of South Dakota Foundation for use of xenon. We also acknowledge the University of Alabama for providing xenon.

[1] D. S. Akerib *et al.* (LZ Collaboration), Nucl. Instrum. Methods Phys. Res., Sect. A **953**, 163047 (2020).
[2] E. Aprile *et al.* (XENON Collaboration), Phys. Rev. Lett. **131**, 041003 (2023).
[3] Y. Meng *et al.* (PandaX-4T Collaboration), Phys. Rev. Lett. **127**, 261802 (2021).
[4] J. Aalbers *et al.* (LZ Collaboration), Phys. Rev. Lett. **131**, 041002 (2023).
[5] J. Fan, M. Reece, and L.-T. Wang, J. Cosmol. Astropart. Phys. 11 (2010) 042.
[6] A. L. Fitzpatrick, W. Haxton, E. Katz, N. Lubbers, and Y. Xu, J. Cosmol. Astropart. Phys. 02 (2013) 004.
[7] D. Akerib *et al.* (LUX Collaboration), Phys. Rev. D **104**, 062005 (2021).
[8] E. Aprile *et al.* (XENON Collaboration), Nature (London) **568**, 532 (2019).
[9] J. Xia, W. C. Haxton *et al.* (PandaX Collaboration), Phys. Lett. B **792**, 193 (2019).
[10] J. Aalbers *et al.* (LZ Collaboration), Phys. Rev. D **109**, 092003 (2024).
[11] P. Agrawal *et al.*, Eur. Phys. J. C **81**, 1015 (2021).
[12] N. Anand, A. L. Fitzpatrick, and W. C. Haxton, Phys. Rev. C **89**, 065501 (2014).
[13] B. J. Mount *et al.* (LZ Collaboration), arXiv:1703.09144.
[14] M. Szydagis *et al.* (NEST Collaboration), Noble element simulation technique (2022), 10.5281/zenodo.6534007.
[15] M. Szydagis *et al.*, arXiv:2211.10726.
[16] I. Jeong, S. Kang, S. Scopel, and G. Tomar, Comput. Phys. Commun. **276**, 108342 (2022).
[17] J. Menéndez, A. Poves, E. Caurier, and F. Nowacki, Nucl. Phys. **A818**, 139 (2009).
[18] A. L. Fitzpatrick, W. C. Haxton, C. W. Johnson, and K. S. McElvain (to be published).
[19] D. Baxter *et al.*, Eur. Phys. J. C **81**, 907 (2021).
[20] R. Schoenrich, J. Binney, and W. Dehnen, Mon. Not. R. Astron. Soc. **403**, 1829 (2010).
[21] J. Bland-Hawthorn and O. Gerhard, Annu. Rev. Astron. Astrophys. **54**, 529 (2016).
[22] R. Abuter *et al.* (GRAVITY Collaboration), Astron. Astrophys. **647**, A59 (2021).
[23] M. C. Smith *et al.*, Mon. Not. R. Astron. Soc. **379**, 755 (2007).
[24] J. Lewin and P. Smith, Astropart. Phys. **6**, 87 (1996).
[25] See Supplemental Material at http://link.aps.org/supplemental/10.1103/PhysRevLett.133.221801 for data release for this result.
[26] P. Faulkner *et al.*, J. Phys. G **32**, N1 (2005).
[27] D. Britton *et al.*, Phil. Trans. R. Soc. A **367**, 2447 (2009).